Cell Stem Cell, Volume *32*

Supplemental Information

Integrating collecting systems in human kidney organoids through fusion of distal nephron to ureteric bud

Min Shi, Brittney Crouse, Nambirajan Sundaram, Naomi Pode Shakked, Konrad Thorner, Nathaniel M. King, Parna Dutta, Lioba Ester, Weitao Zhang, Vinothini Govindarajah, Raphael Kopan, Cristina Cebrian, Christopher N. Mayhew, Michael A. Helmrath, Joseph V. Bonventre, and Kyle W. McCracken

Table S1. Conditions and cell counts for scRNA-seq experiments. Related to STAR Methods.

Sample	Day	Composition	Condition	No. Cells	Figure
1	**0**	**Mixed**	**Control**	**5,655**	Supp. Fig. 3
			Epithelial Subset	*3,533*	Fig. 1-3, Supp. Fig. 4-6
			UB Subset	*910*	Fig. 7, Supp. Fig. 9
2	**3**	**NM Only**	**Control**	**10,523**	
			Epithelial Subset	*7,577*	Fig. 3F
3	**3**	**Mixed**	**Control**	**10,116**	Supp. Fig. 3
			Epithelial Subset	*7,106*	Fig. 1-3, Supp. Fig. 4-6
			UB Subset	*1,592*	Fig. 7, Supp. Fig. 9
4	**7**	**NM Only**	**Control**	**9,018**	
			Epithelial Subset	*7,652*	Fig. 3F
5	**7**	**Mixed**	**Control**	**8,676**	Supp. Fig. 3
			Epithelial Subset	*6,703*	Fig. 1-3, Supp. Fig. 4-6
			UB Subset	*785*	Fig. 7, Supp. Fig. 9
6	**10**	**Mixed**	**Control**	**10,179**	Fig. 3H, Supp. Fig. 3
			Epithelial Subset	*6,523*	Fig. 1-3, Supp. Fig. 4-6
			UB Subset	*456*	Fig. 7, Supp. Fig. 9
7	**14**	**NM Only**	**Control**	**9,515**	
			Epithelial Subset	*7,049*	Fig. 2-3, Supp. Fig. 5-6
8	**14**	**Mixed**	**Control**	**11,078**	Fig. 3H, Supp. Fig. 3
			Epithelial Subset	*7,309*	Fig. 1-3 & 5, Supp. Fig. 4-6
			UB Subset	*452*	Fig. 7, Supp. Fig. 9
9	**14**	**Mixed**	**DAPT (d4-6)**	**10,601**	
			Epithelial Subset	*6,061*	Fig. 5
10	**14**	**Mixed**	**CDM (d10-14)**	**9,142**	
			Epithelial Subset	*5,611*	Fig. 7, Supp. Fig. 10
11	**14**	**Mixed**	**CDM+AUX**	**17,512**	Fig. 7, Supp. Fig. 10
			Epithelial Subset	*12,017*	Fig. 7, Supp. Fig. 10
12	**14**	**UB Only**	**CDM + AUX**	**10,804**	
			Epithelial Subset	*1,964*	Supp. Fig. 9F-H
			Total	**122,819**	

Table S2. Comparison of scRNA-seq across organoid datasets. Related to Figure 7.

		Organoid Dataset			
		Shi	**Uchimura**	**Vanslambrouck**	**Phipson**
	Stage	Day 14 (22)	Day 26	Day 13+14 (27)	Day 25
	Total Cells	17,512	15,301	13,995	6,373
LineageID	Nephron	62.09%	7.17%	32.67%	9.78%
	UrEp	4.35%	20.16%	0.00%	0.02%
	Stroma	22.38%	47.76%	52.75%	62.09%
	NPC-like	0.09%	9.25%	1.46%	8.22%
	Endo	0.05%	0.00%	0.37%	7.94%
	unassigned	11.05%	15.67%	12.72%	11.96%
Nephron Segment	Podocyte	22.40%	3.10%	1.60%	9.60%
	Prox Tub	23.77%	2.95%	17.13%	0.20%
	LOH/TAL	3.84%	1.78%	5.13%	0.13%
	Dist Tub	12.36%	7.89%	8.46%	1.58%
	Col Duct	6.36%	17.17%	0.13%	1.35%

Table S3. Statistical tests and p-values. Related to STAR Methods.

Figure	Group	N	Comparison	*P* value	Test
Fig. 5C	Control (HNF4A-mScarlet)	4			
	Day 4 - 6 (HNF4A-mScarlet)	4	Control vs. Day 4 - 6 (*HNF4A*-mScarlet)	0.24655	Unpaired Student's *t*-test
	Day 3 - 6 (HNF4A-mScarlet)	4	Control vs. Day 3 - 6 (*HNF4A*-mScarlet)	<0.0001	Unpaired Student's *t*-test
	Day 2 - 6 (HNF4A-mScarlet)	4	Control vs. Day 2 - 6 (*HNF4A*-mScarlet)	0.0005	Unpaired Welch's *t*-test
	Control (GATA3-mScarlet)	4			
	Day 4 - 6 (GATA3-mScarlet)	4	Control vs. Day 4 - 6 (*GATA3*-mScarlet)	0.0024	Unpaired Student's *t*-test
	Day 3 - 6 (GATA3-mScarlet)	4	Control vs. Day 3 - 6 (*GATA3*-mScarlet)	0.016	Unpaired Welch's *t*-test
	Day 2 - 6 (GATA3-mScarlet)	4	Control vs. Day 2 - 6 (*GATA3*-mScarlet)	0.0037	Unpaired Welch's *t*-test
Fig. 5H	Control	3	Control vs. +DAPT	0.001	Unpaired Student's *t*-test
	+DAPT	3			
Fig. 5I	Control	6	Control vs. +DAPT	0.045	Unpaired Student's *t*-test
	+DAPT	6			
Fig. 6B	Control	4	Control vs. +XAV	0.0055	Unpaired Student's *t*-test
	+XAV	4			
Fig. 6D	Control	8	Control vs. +Dox	0.0392	Unpaired Welch's *t*-test
	+Dox	8			
Fig. 6E	Control	3	Control vs. +Dox	0.0485	Unpaired Student's *t*-test
	+Dox	3			
Fig. 6H	Control	4	Control vs. +Dox	0.0041	Unpaired Welch's *t*-test
	+Dox	4			
	+XAV	4	XAV vs. +Dox	0.0082	Unpaired Welch's *t*-test
	+XAV+Dox	4			
Fig. 6I	Control	4	Control vs. +Dox	0.489	Unpaired Student's *t*-test
	+Dox	4			
	+XAV	4	XAV vs. +Dox	0.0076	Unpaired Student's *t*-test
	+XAV+Dox	4			
Supp. Fig. 8A	Control	3			
	+XAV	3	Control vs. +XAV	0.0056	Unpaired Student's *t*-test
	+CHIR	3	Control vs. +CHIR	<0.0001	Unpaired Student's *t*-test
Supp. Fig. 8B	Control	3	HNF4A (XAV)	0.0466	Unpaired Student's *t*-test
	+XAV	3	HNF4A (CHIR)	0.0255	Unpaired Welch's *t*-test
	+CHIR	3	NPHS1 (XAV)	0.2253	Unpaired Student's *t*-test
			NPHS1 (CHIR)	0.0141	Unpaired Welch's *t*-test
			NPHS2 (XAV)	0.1708	Unpaired Student's *t*-test
			NPHS2 (CHIR)	0.0111	Unpaired Welch's *t*-test
			CALB1 (XAV)	0.0214	Unpaired Student's *t*-test
			CALB1 (CHIR)	0.0152	Unpaired Welch's *t*-test

			SLC12A1 (XAV)	0.4928	Unpaired Student's *t*-test
			SLC12A1 (CHIR)	0.0008	Unpaired Student's *t*-test
			CDH1 (XAV)	0.0775	Unpaired Student's *t*-test
			CDH1 (CHIR)	0.1601	Unpaired Welch's *t*-test
Supp. Fig. 8C	Control	3	Control vs. +Dox	0.0236	Unpaired Student's *t*-test
	+Dox	3			
Supp. Fig. 9D	Control	3	Control vs. CDM + AUX (*AQP2*)	0.0001	One-way ANOVA and Tukey's test
	CDM	3	CDM vs. CDM + AUX (*AQP2*)	0.0005	One-way ANOVA and Tukey's test
	CDM + AUX	3	Control vs. CDM + AUX (*ELF5*)	0.0025	One-way ANOVA and Tukey's test
			CDM vs. CDM + AUX (*ELF5*)	0.0015	One-way ANOVA and Tukey's test
			Control vs. CDM + AUX (*SCNN1G*)	0.0175	One-way ANOVA and Tukey's test
			CDM vs. CDM + AUX (*SCNN1G*)	0.0048	One-way ANOVA and Tukey's test

Table S4. qPCR Primers. Related to STAR Methods.

Gene	Forward primer	Reverse primer
AQP2	CACGTCTCCGTTCTCCGAG	CTGTTGCTGAGAGCATTGACA
CALB1	TGTGGATCAGTATGGGCAAAGA	CTCAGTTTCTATGAAGCCACTGT
CDH1	CGAGAGCTACACGTTCACGG	GGGTGTCGAGGGAAAAATAGG
CITED1	GCTGGCTAGTATGCACCTGC	CATTGGCTCGGTCCAACCC
ELF5	TAGGGAACAAGGAATTTTTCGGG	GTACACTAACCTTCGGTCAACC
GAPDH	CCCATCACCATCTTCCAGGAG	CTTCTCCATGGTGGTGAAGACG
HNF4A	CGAAGGTCAAGCTATGAGGACA	ATCTGCGATGCTGGCAATCT
NPHS1	CTGCCTGAAAACCTGACGGT	GACCTGGCACTCATACTCCG
NPHS2	ACCAAATCCTCCGGCTTAGG	CAACCTTTACGCAGAACCAGA
PPIA	CCCACCGTGTTCTTCGACATT	GGACCCGTATGCTTTAGGATGA
SCNN1G	GCACCCGGAGAGAAGATCAAA	TACCACCGCATCAGCTCTTTA
SLC12A1	GCCAGTTTTCACGCTTATGATTC	CTATCTTGGGAACGGCATCCA
SIX2	CCTGCGAGCACCTTCACAA	CTCGATGTAGTGTGCCTTGAG
RET	ACACGGCTGCATGAGAACAA	GCCCTCACGAAGGGATGTG
WNT11	GACCTCAAGACCCGATACCTG	TAGACGAGTTCCGAGTCCTTC

Supplementary Figure Legends

Figure S1. Differentiation strategies for generating NM and UB progenitor cells, Related to Figure 1. A. NM was induced in monolayer format and used to make organoids at day 8. **B.** The cultures expressed key nephron progenitor markers including SIX2, SIX1, and PAX2. **C.** UB spheroids were generated through aggregation of pronephric intermediate mesoderm progenitors at day 3 of differentiation, and the spheroids were used to assemble organoids at day 6. **D.** The spheroids at day 7 comprised both UB and stromal progenitor populations as indicated in scRNA-seq analysis, with the former exhibiting high expression of the tip markers *RET*, *WNT11*, and *ETV4/5*. Scale bar, 200 μm (B).

Figure S2. Optimization of growth conditions for recombinant kidney organoids, Related to Figure 1. A. Addition of ROCK inhibitor Y-27632 for the first 5 hours post-mixing promoted efficient aggregation of progenitor cells and more consistent induction and epithelialization of the NM by day 4. **B.** Transient BMP inhibition (with LDN) between days 0-2 led to improved efficiency of NM induction and UB growth. **C.** qPCR analyses confirmed loss of undifferentiated NPC markers *SIX2* and *CITED1* from day 0 to day 4 and reduction of UB tip progenitor markers *RET* and *WNT11*. *n*=3 organoid replicates per timepoint. **D.** Organoids generated from UBs harboring a *GATA3*-mScarlet reporter allele mixed with unlabeled (H1-derived) NM enabled visualization of the growth of the UB epithelia without seeing the UB spheroid-derived stroma. **E.** Whole-mount staining of organoids at days 0, 2, and 4 indicated that the presence of UB progenitors did not affect the rapid induction of JAG1 or the gradual extinction of SIX1 expression. **F.** Neither addition of FGF2 nor GDNF altered renal vesicle formation or UB branching by day 4, and they did not affect the differentiation of organoids by day 14. Scale bars, 500 μm (A, D), 1,000 μm (B, F), 200 μm (E).

Figure S3. Single cell profiling of kidney organoid development, Related to Figure 1. A-B. UMAP embedding identified 28 cell clusters spanning days 0, 3, 7, 10, and 14 of differentiation. **C-D**. Integrating both supervised and unsupervised annotation showed the organoids comprised multiple lineages, including NPC and Nephron, Ureteric, Stromal, and off-target neural-like cells with enriched expression of *SOX2* and *MAP2*. **E**. Feature plot showing unsupervised *DevKidCC* lineage prediction scores for Ureteric (UrEp), NPC, Nephron, and Stroma. **F**. Canonical marker expression was used to corroborate *DevKidCC* lineage assignments. **G**. Reference mapping of the organoid cells (from days 0-14) to a human fetal kidney reference dataset[22] showed general agreement in annotation of both nephron/epithelial and stromal cell types.

Figure S4. Reclustering and analysis of nephron and ureteric lineages, Related to Figure 2. A. 19 clusters were identified to represent NM and UB lineage differentiation across 14 days of differentiation. **B**. Expression of GFP was specific to clusters 7, 9, and 13, which were annotated as UB lineage in Fig. 1F. **C**. *DevKidCC* was used to assign unsupervised annotations across this dataset, with prediction scores shown for NPC, early nephron (EN), early podocyte (EPod), podocyte, parietal epithelial cell (PEC), early proximal tubule (EPT), early distal tubule (EDT), loop of Henle (LOH), distal tubule (DT), and ureteric epithelium (UrEp). **D**. Expression of representative genes identifying early stages of NM lineage differentiation. **E**. Violin plot showing expression of anchor genes associated with each cell type shown in Fig. 1E.

Figure S5. Formation of collecting ducts in Mixed organoids, Related to Figure 2. A. Expression of CD markers were either enriched (*GATA3*) or exclusive (*CALB1*, *ELF5*, *AQP2*, *SCNN1G*) to Mixed organoids made with UB progenitors compared to NM Only organoids. These genes were found in the CD cluster shown in Fig. 2A. **B**. Similarly, these cells were identified as ureteric epithelium (UrEp) by *DevKidCC*, whereas the remaining cells and all of those in NM organoids were identified as Nephron-derived. **C**. Wholemount staining demonstrated the continuous luminal connection across the junction of the GFP^+ CD and GFP^- nephron tubule. **D.** $HNF4A^+$ proximal tubules represented most NM-derived epithelial tissue in the organoids, while $GATA3^+$ (GFP^-) distal nephrons were far less abundant at day 14. **E.** *GATA3*-mScarlet expression in the nephron lineage was first weakly detected as early as day 5 in small domains of renal vesicles (yellow arrows), and by day 7 it was strongly expressed in the presumptive distal segments of nascent nephrons. By day 14, the distal tubules were frequently fused to the GFP^+ CDs. **F.** IF staining for GATA3 and TJP1 revealed that more than one $GATA3^+$ distal tubules connected into a single GFP^+ ureteric tubule by day 7. Scale bars, 100 μm (C, F), 1,000 μm (D, E).

Figure S6. Analysis of proximal nephron and stromal components of organoids, Related to Figure 3. **A-B**. Annotated cell types of the epithelial components of both Mixed and NM organoids (combined) at day 14

closely aligned with both unsupervised DevKidCC segment assignment scoring (**A**) and canonical anchor gene expression (**B**). **C**. Functional transport assay demonstrated that organoid proximal tubules uptake (secrete) 6-carboxyfluorescein following 1 hour incubation. **D**. A higher number of GATA3-expressing connecting segment cells were observed in the NM-derived distal tubule (CD cluster removed from plots) in the Mixed organoids compared to NM only. **E**. Overall, there were no marked qualitative differences in marker gene expression associated with nephron segments in Mixed vs. NM Only organoids, although most of LOH/TAL genes were consistently more highly expressed in the Mixed organoids. Neither condition exhibited *SLC12A3* expression in the distal tubule clusters. **F**. Comparison of interstitial cell gene expression in the GFP^+ vs GFP^- cells in the stromal cluster (Fig. 3H) revealed no substantive differences, suggesting that comparable stromal populations arise from both the NM and UB differentiations. Scale bar, 1,000 μm (C).

Figure S7. NOTCH inhibition enhances distal nephron development and fusion, Related to Figure 5. A. Exposure to DAPT from days 2-6 or 3-6 led to expansion of *GATA3* expressing tubules and nearly complete repression of podocytes (NPHS1) by day 14, whereas treatment from days 4-6 increased the distal nephron specification but maintained similar levels of proximal structures such as podocytes. **B.** The $GATA3^+$ segments in DAPT-treated organoids formed normal patent anastomoses with the UB-derived CDs, and they frequently expressed the connecting segment marker CALB1. Scale bars, 1,000 μm (A), 200 μm (B).

Figure S8. Testing WNT and GATA3 in nephron segmentation and fusion, Related to Figure 6. A. Quantification of GATA3-$mScarlet^+$ area (from Fig. 6A) revealed a dose-dependent WNT response, where activation (CHIR) and inhibition (XAV) led to significant increase and decrease in GATA3 expression in the NM lineage, respectively. *n*=3 independent biological replicates per condition; column and error bars represent mean and standard deviation, respectively; $^{**}P = 0.0056$, $^{****}P < 0.001$. **B**. Expression analysis of day 14 organoids by qPCR showed that proximal segment markers (*HNF4A*, *NPHS1*, *NPHS2*) exhibited the opposite pattern, with suppression by CHIR and variable increase induced by XAV. The more distal nephron markers *CALB1* and *SLC12A1* were increased by WNT activation. *n*=3 independent biological replicates per condition; column and error bars represent mean and standard deviation, respectively; $^{*}P < 0.05$, $^{***}P < 0.001$. **C.** The dox-inducible WNT9B cassette was stably introduced to hPSCs using the pInducer20 lentivirus. In the undifferentiated cells, addition of doxycycline led to significant activation of *WNT9B* measured by qPCR. *n*=3 independent biological replicates per condition; column and error bars represent mean and standard deviation, respectively; $^{*}P = 0.0236$. **D**. Wholemount staining of control and Dox-treated organoids showed that UB-derived *WNT9B* activation led to increased GATA3 expression in the NM lineage and more fusion events (as quantified in Fig. 6D-E). **E**. The dox-inducible GATA3 cassette was similarly introduced to hPSCs through the pInducer20 lentivirus. Exposure to doxycycline for 24 hours induced mosaic expression of GATA3 in the undifferentiated hPSCs. **F**. Wholemount staining of GATA3 in the NM lineage with UB expression digitally subtracted based on overlap with expression of the GFP reporter. Addition of Dox led to mosaic and sometimes patchy expression of GATA3 within the organoids. XAV treated (WNT inhibited) organoids exhibited markedly reduced GATA3 expression in the NM lineage, which was rescued by transgene activation. Scale bars, 1,000 μm (D, F), 200 μm (E).

Figure S9. Interrogating CD maturation in UB-derived epithelia, Related to Figure 7. A. Violin plot expression of UB lineage markers across the differentiation from days 0-14, as shown in feature plots in Fig. 7B. More differentiated principal cell markers were induced by days 10-14, but expression of *AQP2* remained low. **B**. The expression of *AQP2* was induced in UB epithelia grown either in isolation or in recombinant organoids with NM when cultured in previously identified conditions to grow UB organoids (UB Medium), but not when grown in the minimal 'Mix' media. **C**. Schematic representation of methods for growing UB organoids in isolation in 3D culture and their differentiation to $AQP2^+$ cells following exposure to a minimal 'CD Medium'. Following transition to CD Medium, activation of either the WNT (CHIR99021), FGF/GDNF, or TGFβ (Activin A) pathways was sufficient to repress activation of the *AQP2* reporter allele, while RA and BMP4 had no appreciable effect. **D**. CD Medium (CDM) induced higher expression of *AQP2*, *ELF5*, and *SCNN1G* in Mixed organoids at day 14, and they were significantly further augmented by the addition of A83, U0126, and XAV. *n*=3 independent biological replicates per condition; column and error bars represent mean and standard deviation, respectively; P-values shown in figure. **E**. AQP2 was induced by AUX specifically within the GFP^+ UB-derived CDs. **F**. The overall morphology and architecture of organoids at day 14 was unaffected by transition to CD Medium (CDM) or CDM + AUX (A83, U0126, XAV939) culture medium, and the formation of UB-derived CD-like tubules and nephron fusion via $GATA3^+$ segments were preserved. **G**. UMAP embedding of epithelial components of both Mixed (including Control, CDM, and CDM+AUX conditions) and UB Only (CDM+AUX condition) organoids at

day 14. **H**. The CD-like cells from UB Only organoids clustered distinctly from those in Mixed organoids. **I**. Expression of CD principal cell maturation markers was higher in CD cells from Mixed organoids than UB Only organoids. Scale bars, 500 μm (B), 200 μm (C, E), 1,000 μm (F).

Figure S10. Single cell profiling of organoid maturation, Related to Figure 7. A. Single cell profiling at day 14 revealed similar nephron segment distribution among organoids grown in control (Mix Media), CDM, and CDM + AUX conditions from days 10-14. **B**. NM lineage differentiation was largely unaffected by the transition of organoids to CDM or CDM+AUX conditions, with overall similar expression of genes associated with podocyte proximal tubule, LOH/TAL, and distal tubule clusters. **C**. One exception, though, was that CDM+AUX induced a higher level of expression of some genes associated with proximal tubule maturation, such as *SLC34A1*. **D**. Expression of CD principal cell gene expression was highest in the Shi and Uchimura datasets and largely absent in the Vanslambrouck and Phipson organoids. **E**. Markers of intercalated cells were not observed in any of the four single cell datasets.

Supplementary Figure 1

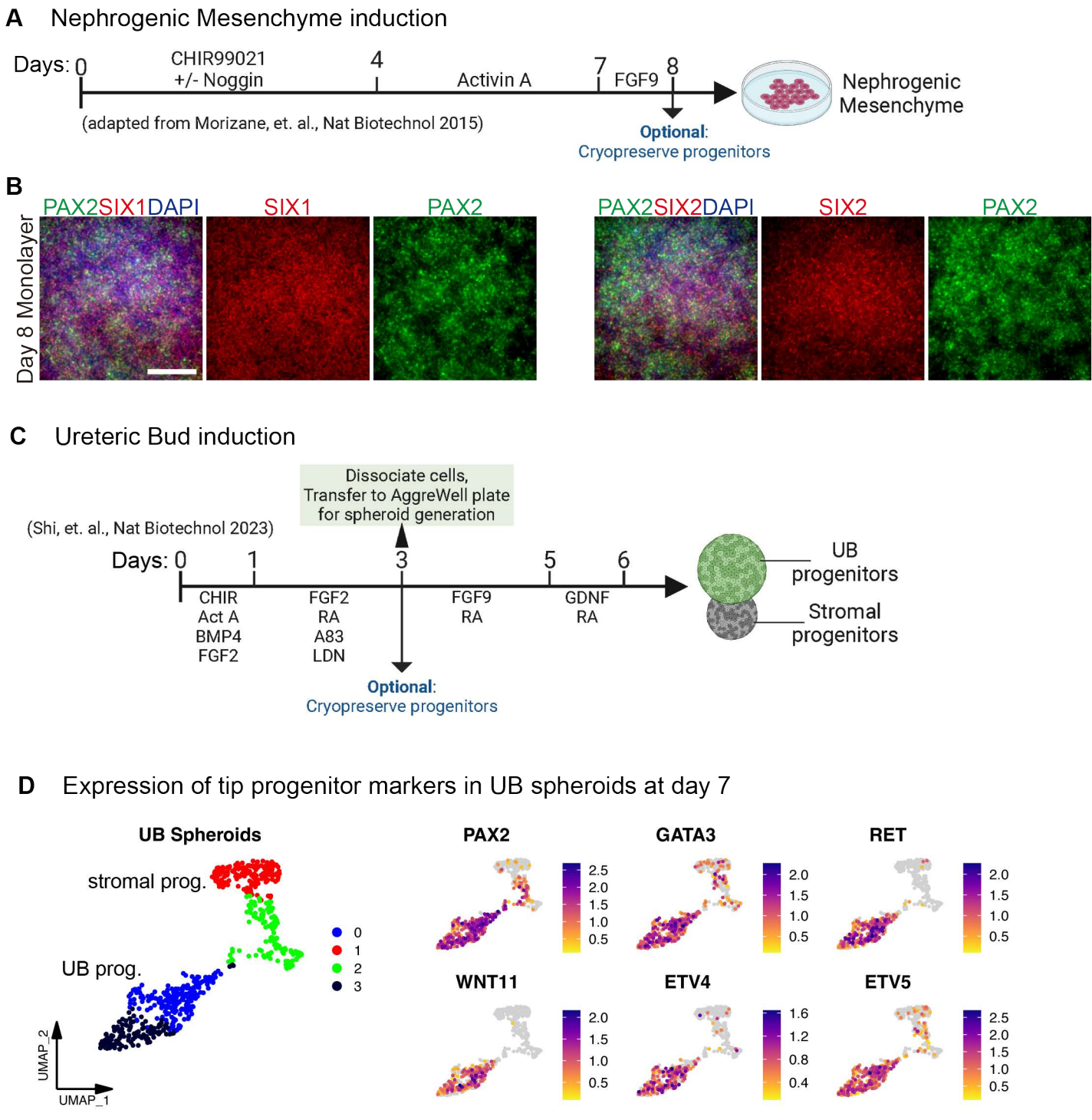

Supplementary Figure 2

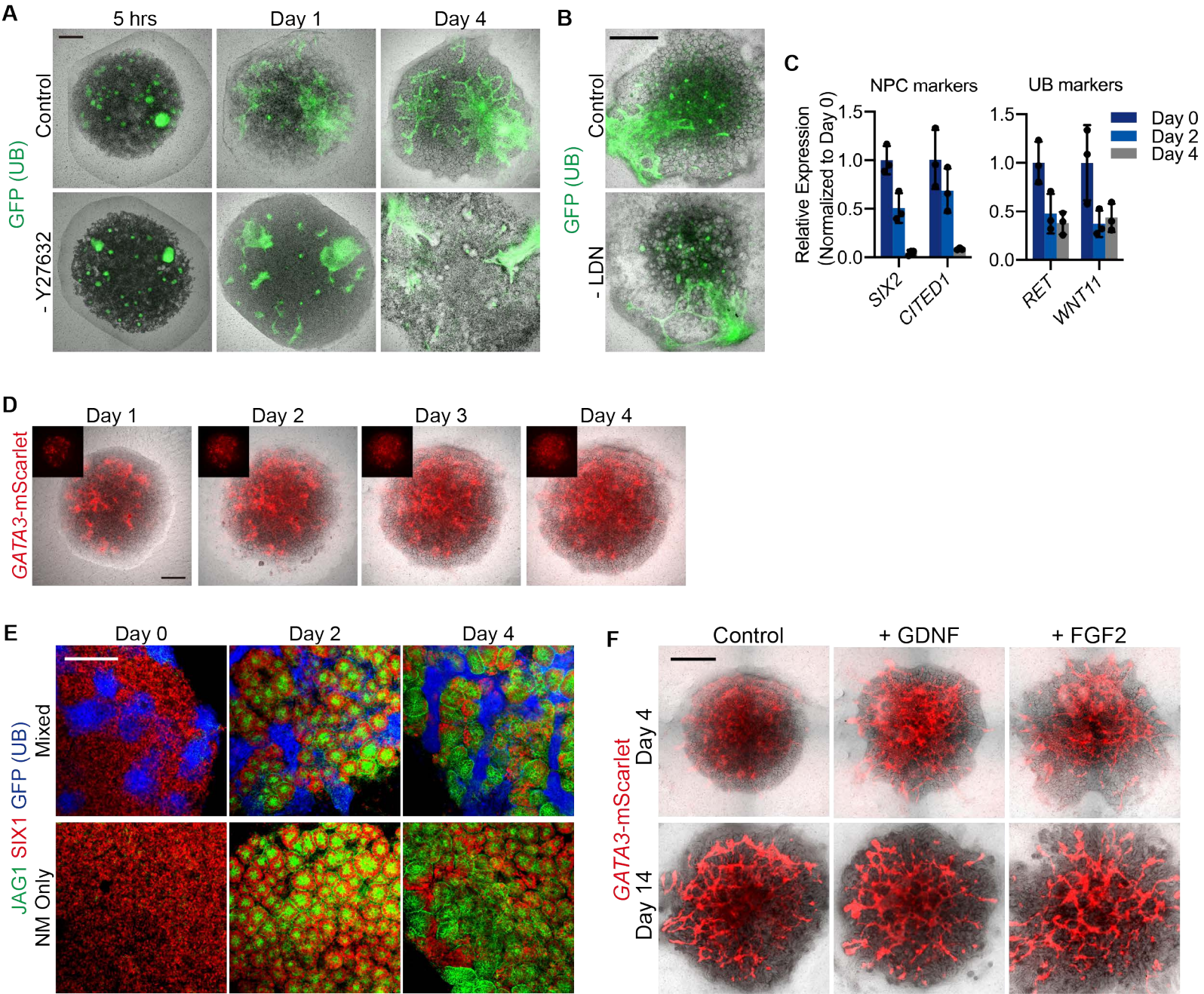

Supplementary Figure 3

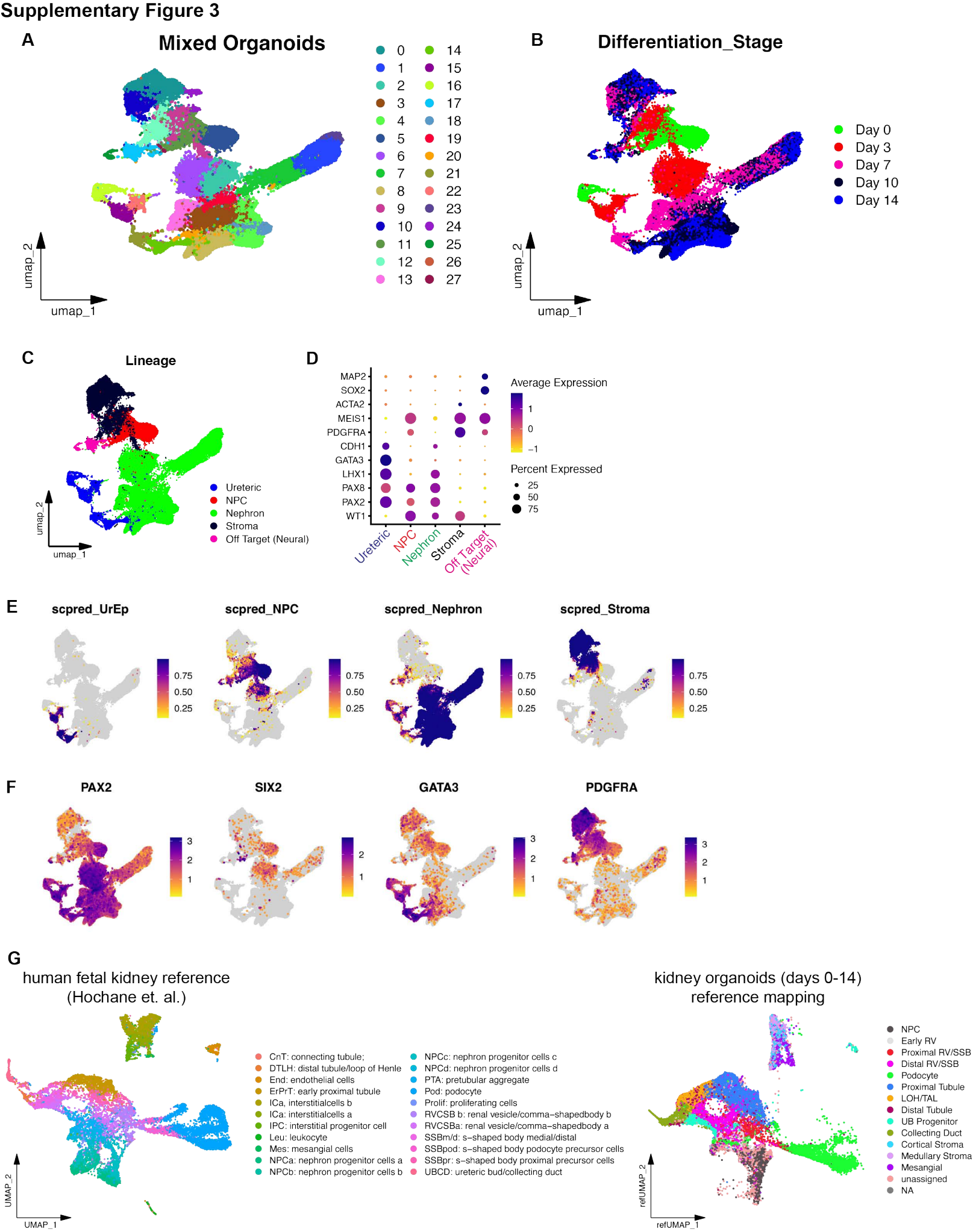

Supplementary Figure 4

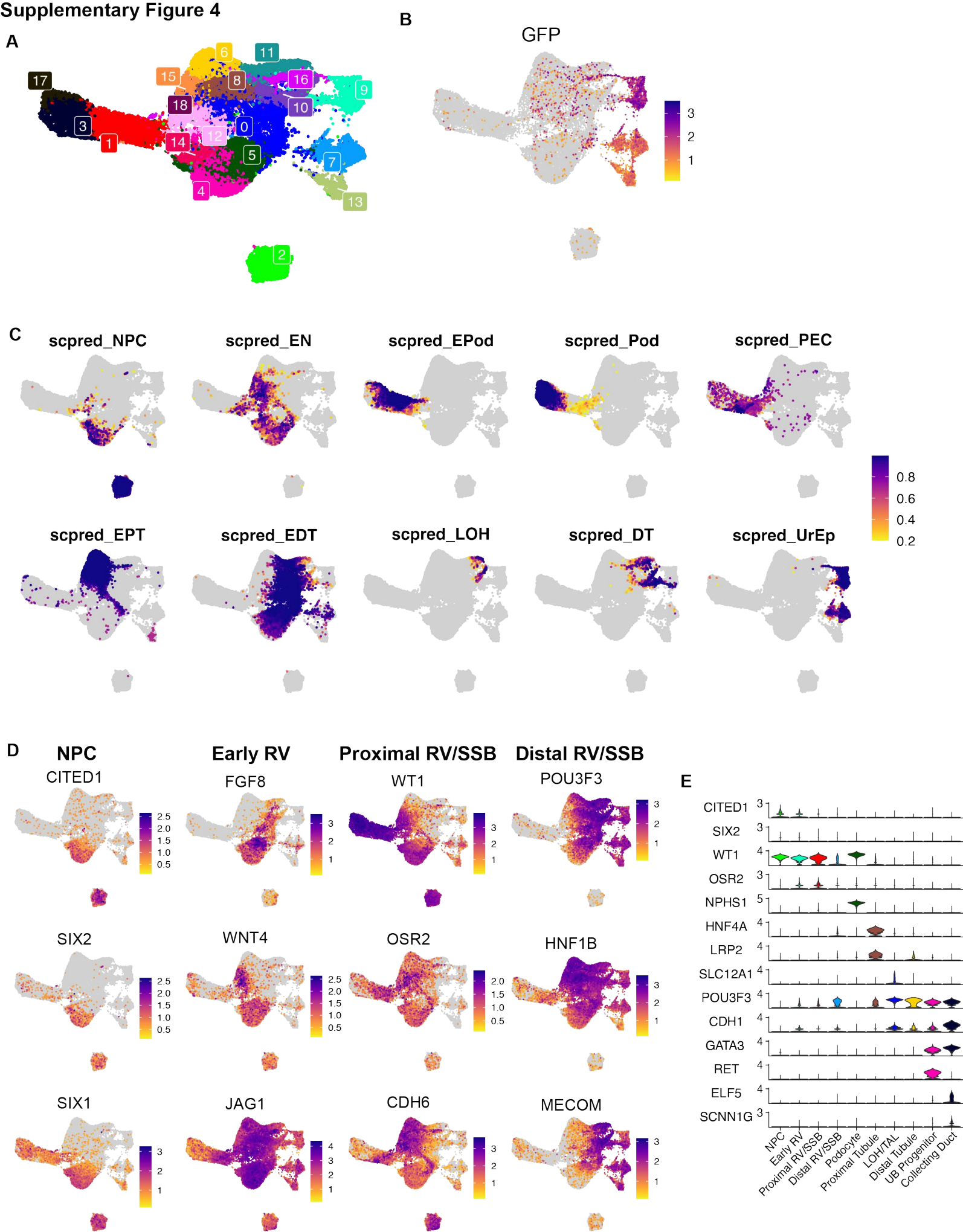

Supplementary Figure 5

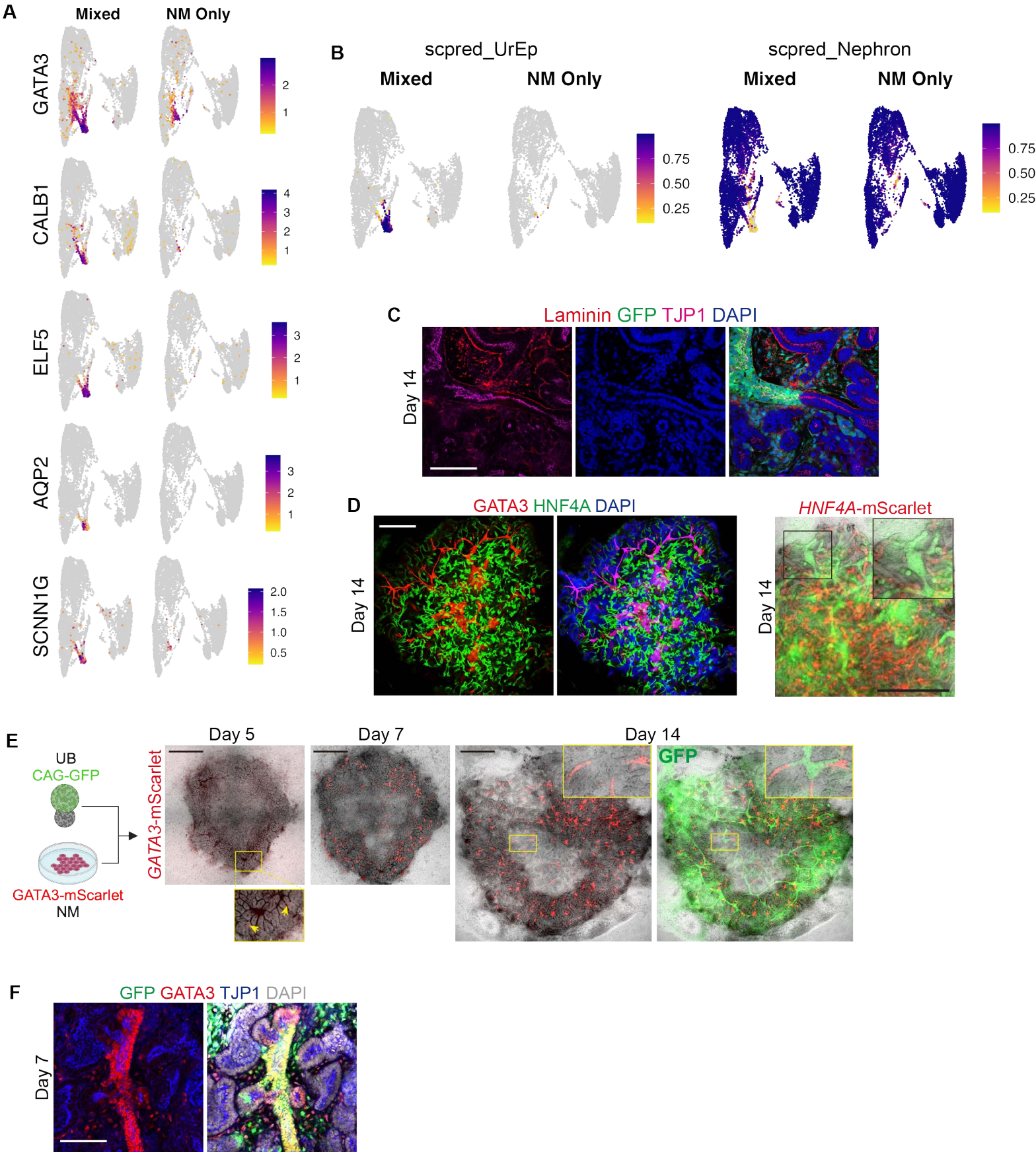

Supplementary Figure 6

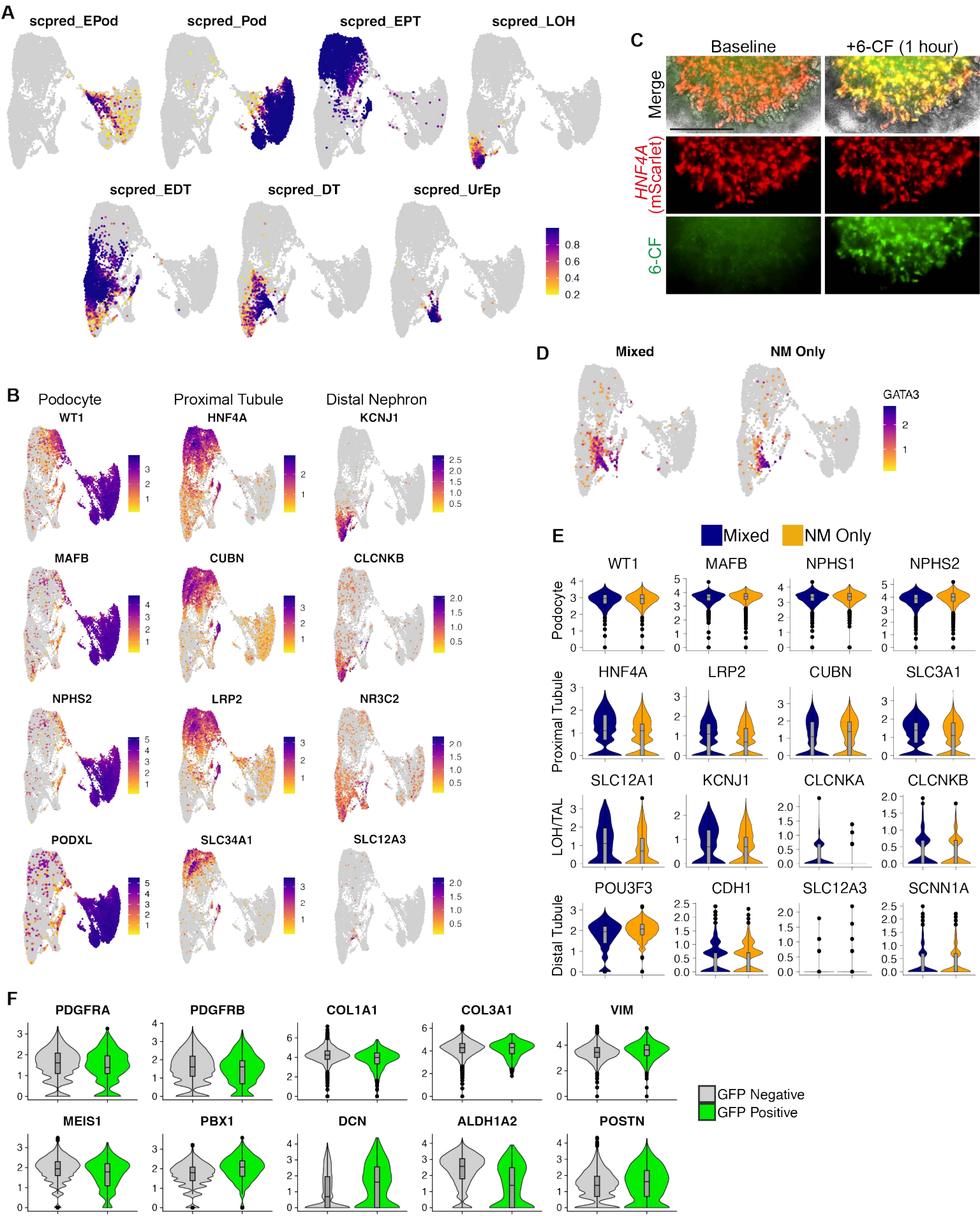

Supplementary Figure 7

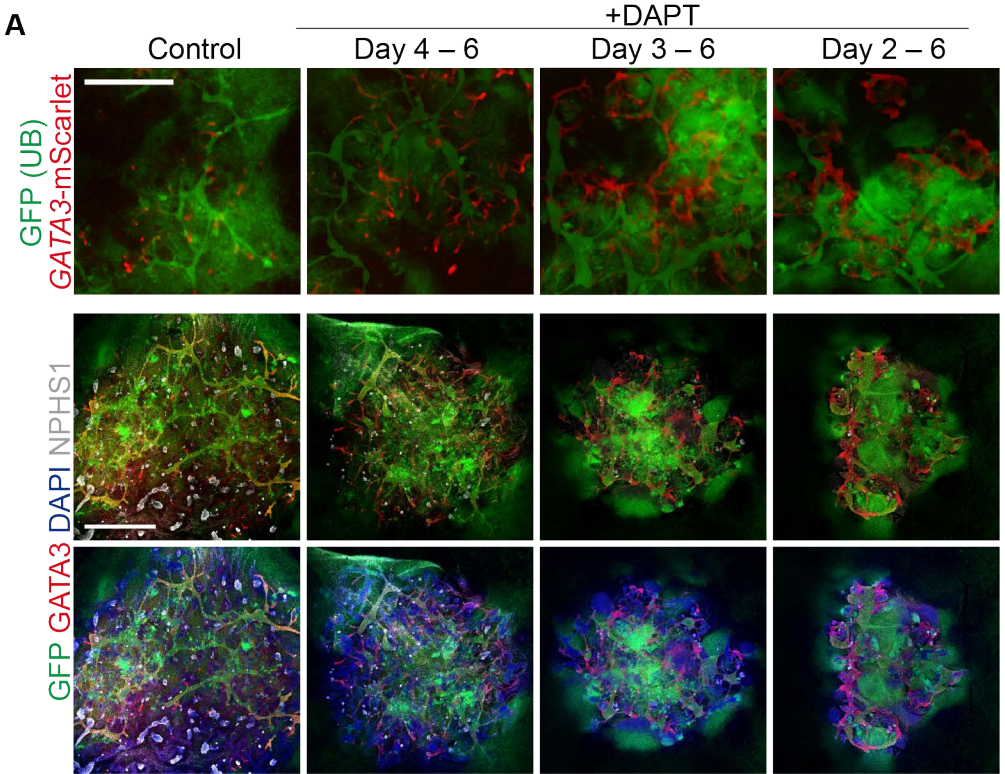

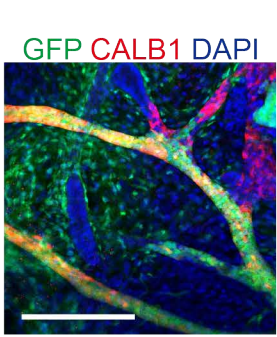

Supplementary Figure 8

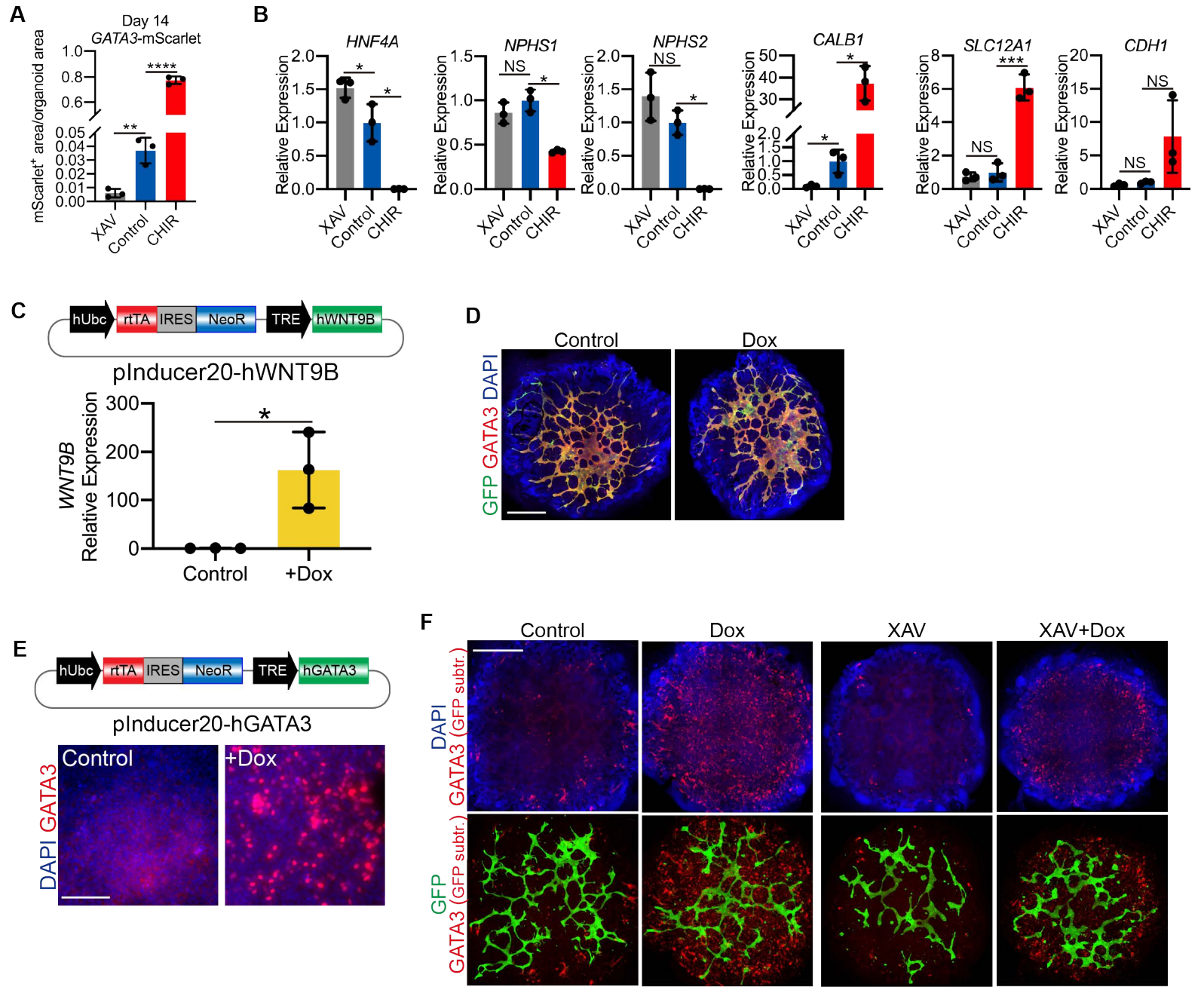

Supplementary Figure 9

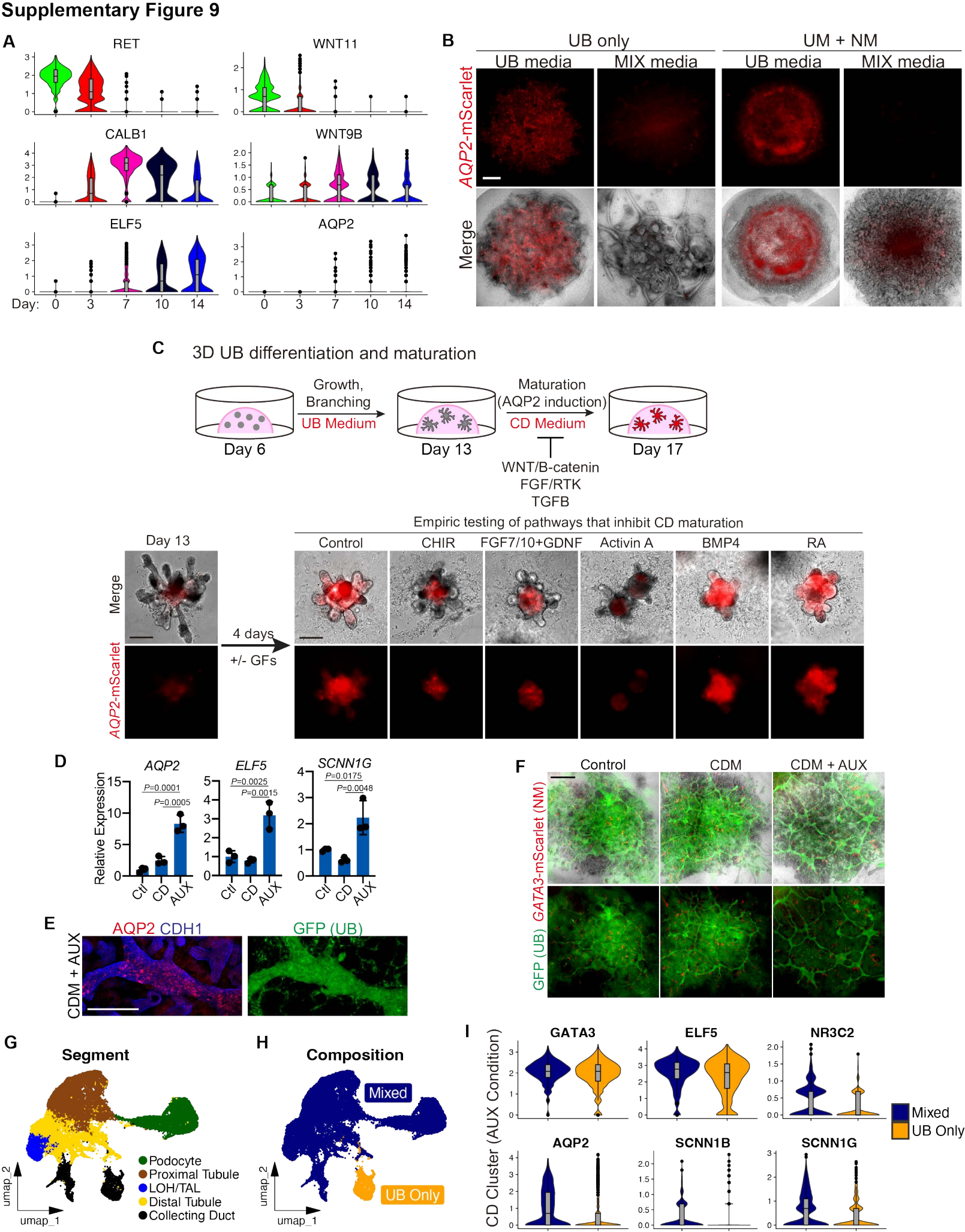

Supplementary Figure 10